

2mm Catheter Design for Endoscopic Optical Coherence Tomography

Kye-Sung Lee¹, Chuck Koehler¹, Eric G. Johnson¹, Eric Valaski TEUMA², Olusegun Ilegbusi², Marco Costa³, Huikai Xie⁴, and Jannick P. Rolland¹

¹CREOL, College of Optics and Photonics, University of Central Florida, 4000 Central Florida Blvd., Orlando FL

²Department of Mechanical, Materials, and Aerospace Engineering, College of Engineering and Computer Science, University of Central Florida, 4000 Central Florida Blvd., Orlando FL

³The Cardiovascular Center, University of Florida Health Science Center, Shands Hospital, Jacksonville, FL

⁴ Department of Electrical and Computer Engineering, University of Florida, Gainesville, FL

ABSTRACT

A biophotonics catheter was conceived with collimation optics, an axicon lens, and custom design imaging optics yielding a 360 degree scan aimed at imaging within concave structures such as arteries and lung lobes. The large depth of focus is necessary to image a long-depth-range sample with constant transverse resolution in optical coherence tomography (OCT). There are two approaches to achieving constant invariant resolution in OCT: Dynamic focusing or Bessel beam formation. This paper focuses on imaging with Bessel beams. The Bessel beams may be created with axicon optics which can be used instead of a conventional focusing lens in the sample arm of the OCT interferometer. In this paper we present the design of a 2mm catheter for optical coherence endoscopy with resolution of about 5 micron across a depth of focus of about 1.6mm. Importantly, we investigated the fabrication of a 800 μ m diameter axicon lens and the associated lateral resolution obtained over a long depth range in our OCT system, compared to the same OCT system using a conventional lens.

Keywords: catheter, optical coherence tomography, axicon, Bessel beam imaging, endoscopy

1. Introduction

Optical coherence tomography (OCT) is a highly sensitive biomedical imaging technique that enables high resolution, cross-sectional imaging in biological tissues and other turbid materials.¹ High axial resolution of OCT is realized by use of a broadband light source whereas the lateral resolution is determined by the numerical aperture of the focusing lens. Although a large numerical aperture of a conventional focusing lens in the sample arm of OCT enables high lateral resolution imaging, a small numerical aperture is required to achieve a large depth of focus (DOF) that allows making a constant transverse resolution image over a long depth range. To overcome this limitation, an axicon lens was recently designed and incorporated into the sample arm of an interferometer to achieve both high lateral resolution and a large DOF simultaneously² and dynamic focusing lenses were used to maintain high transverse resolution over a long depth range.³

Endoscopic optical coherence tomography (EOCT) which combines OCT with endoscopic technique has attracted significant interest because of its high resolution when compared to intravascular ultrasound imaging (IVUS).⁴ An axicon lens can be used as a focusing lens in the narrow endoscope to achieve high lateral resolution over long depth range of imaging because axicon lenses are optical elements that produce a long, narrow focal line along the optical axis instead of the usual focus point of a conventional lens.⁵

In Section 2 of the paper, we demonstrate the diffraction pattern of annular aperture with axicon optics and also describe the relation of the axicon angle with the depth of focus and the lateral resolution over depth. In Section 3, we present

the design of a 2mm catheter for EOCT with a resolution of about 5 micron across a DOF of about 1.6mm. We also report the point spread functions along the depth of focus. In Section 4 we demonstrate the fabrication of an 800 μ m diameter axicon lens. We also present a schematic of a Fourier domain OCT (FD-OCT) used in the experiment. We then incorporated the axicon into the sample arm of the FD-OCT interferometer and investigated the lateral resolution over a long depth range. Results were compared to the same OCT system using a conventional lens.

2. Theory

Recently axicon optics, optical elements that produce focal segments within a specified range, have attracted considerable interest because of their unusual properties and versatility in practical applications.^{6,7} In diffraction theory, the focal segment is characterized by nondiffraction Bessel beams.⁸

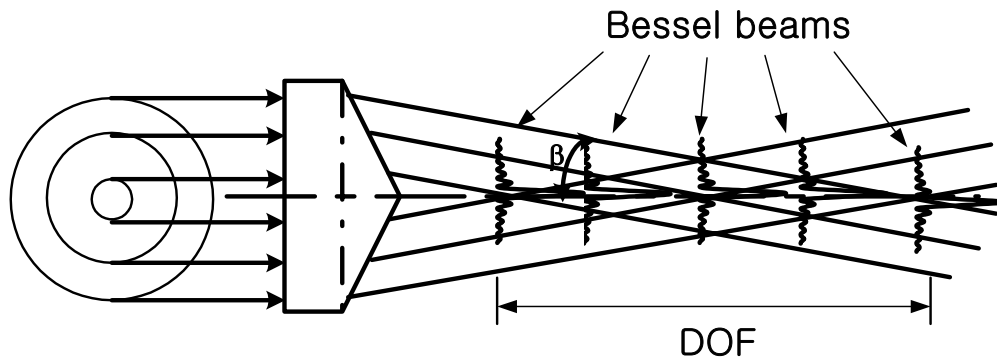


Fig.1. Bessel beams generation with an axicon lens within the focal segment that represents the DOF

Since the J_0 (zero-order Bessel) beam is the Fourier transform of a ring with an infinitively thin width, the conical surface of an axicon generates the diffraction patterns of J_0 beam within the focal segment (i.e. the DOF) as shown in Fig. 1.

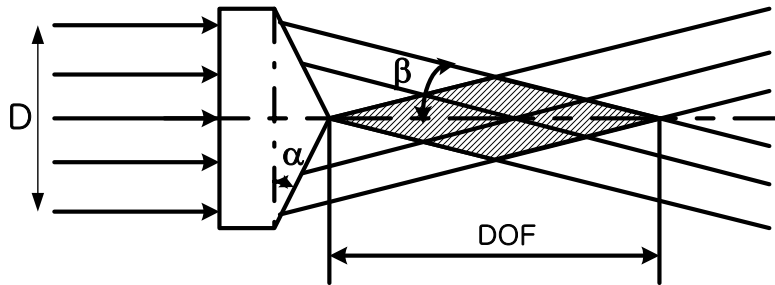


Fig.2. Schematic of an axicon lens

The DOF is defined as the distance from the axicon apex to the geometrical shadow for full-facet illumination and for small angle α of the axicon lens is given as

$$\text{DOF} = \frac{D}{2(n-1)\alpha}, \quad (1)$$

where D denotes the diameter of the collimated incident beam on the axicon lens and n is the refractive index of the axicon lens. The transverse intensity distribution on each focal plane which is generated from each thin annular segment of the collimated incident beam is described by the first order Bessel function. The central lobe size of the first order Bessel is given by

$$\rho_0 = \frac{2.4048\lambda}{2\pi \sin \beta}, \quad (2)$$

where λ is the central wavelength of the incident beam and β is the beam deviation angle with respect to the optical axis of the axicon lens, shown in Fig. 2, which can be calculated as a function of the axicon angle α as

$$\beta = \sin^{-1}(n \sin \alpha) - \alpha \quad (3)$$

The central lobe size ρ_0 is constant in the DOF because the beam focusing angle β is also constant within the geometrical shadow as shown in Fig.2. This property yields a constant lateral resolution within the DOF in OCT.

3. Catheter design

A 2 mm biophotonics catheter was conceived to include collimation optics, an axicon lens, and custom design imaging optics combined with a ~2mm micromotor coupled to a mirror or MEMS to yield a full 360 degree scan within a concave structure such as arteries, lung lobes, and other internal structures. The use of axicon lenses enables a constant resolution in depth scan across about 1.6mm. Resolution of less than 5 micron across a DOF of about 1.6mm was achieved.

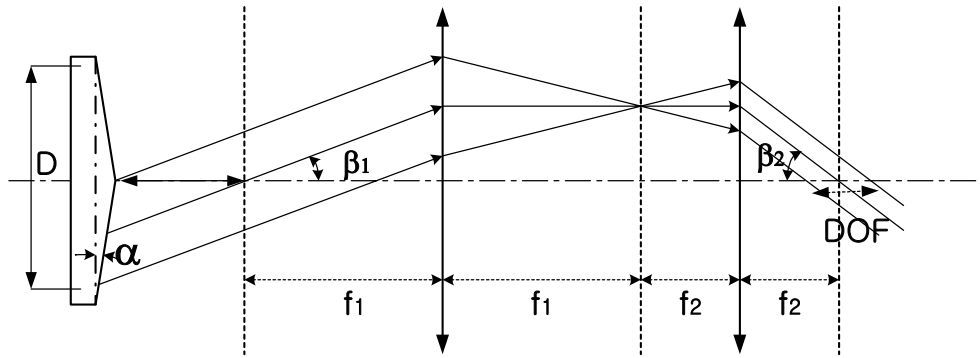


Fig.3. Schematic of 2mm catheter with an axicon and two lenses for relay

Fig. 3 shows the schematic of a 2mm catheter with an axicon and two lenses for relay. The axicon has a 4 degrees axicon angle. The effective focal length (f_1) of first lens is 2mm and the effective focal length (f_2) of the second lens is 1mm. The two lenses relay the DOF generated directly from the axicon to the sample area to be imaged. The two lenses also decrease the DOF size by $(f_1/f_2)^2$ to confine power within a smaller area compared to having no relay lenses, which yields more power efficiency. In addition, the focusing angle β_1 is increased by (f_1/f_2) to β_2 which yields higher resolution (i.e. 5 μm) than before the relay optics as shown in Fig. 3.

<Table 1 parameters and specifications for the 2mm catheter design>

α [degree]	Material of axicon	D [mm]	f1 [mm]	f2 [mm]	DOF [mm]	ρ_0 [μm]
4	fused silica	0.8	2	1	~2	~5

With the parameters and specifications for the 2mm catheter design shown in Table 1, we optimized the design. Fig. 4 shows the layout of the 2mm diameter catheter including an optical fiber, a collimating lens, an axicon lens, a doublet lens, and a 1.9mm micromotor coupled to a MEMS mirror/lens with a shaft and a transparent cover. The MEMS mirror/lens device combines a 45°-tilted mirror and an integrated microlens.⁹ The microlens turns with the spinning shaft of the micromotor to realize 360° real-time focusing. A lateral resolution of 4.8 μm across a DOF of about 1.6mm

was achieved. The catheter was designed and optimized at the three different wavelengths of 750nm, 800nm and 850nm with the weight of 1 2 1 respectively.

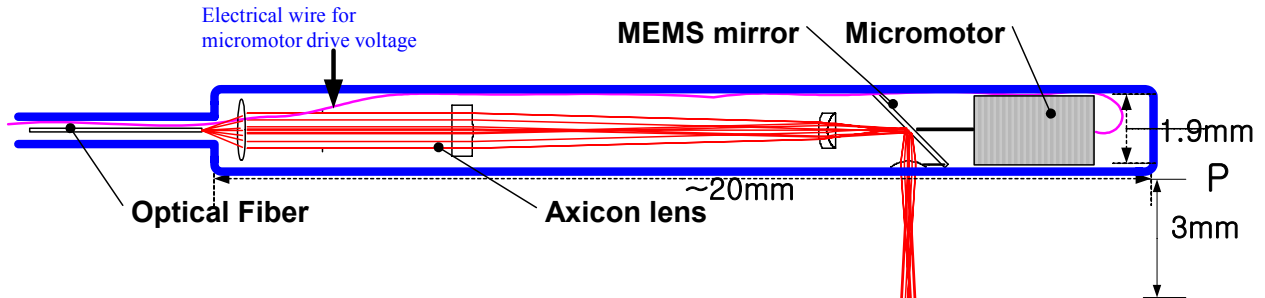


Fig.4. 2D layout of a 2mm diameter catheter

Fig. 5 shows the point spread functions at each focal plane of 1mm, 1.8mm, and 2.6mm from point P shown in Fig. 4. The central lobe sizes of the corresponding point spread functions are $4.8\mu\text{m}$, $4.7\mu\text{m}$, and $5.2\mu\text{m}$.

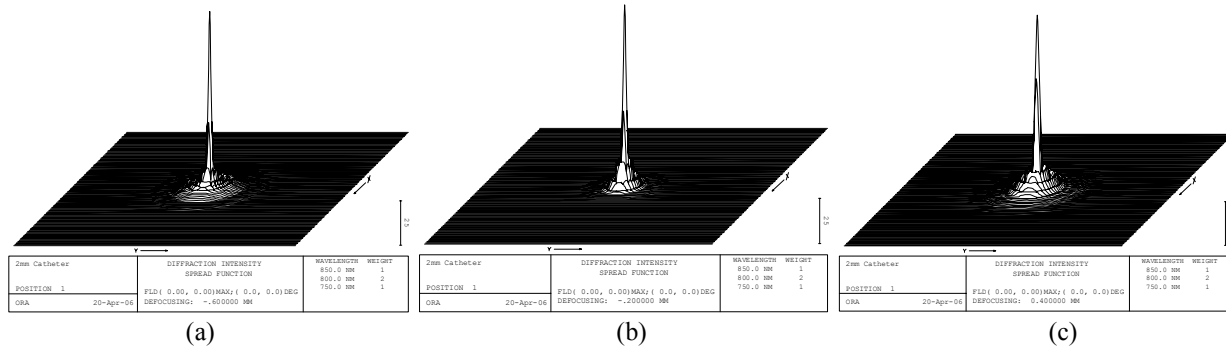
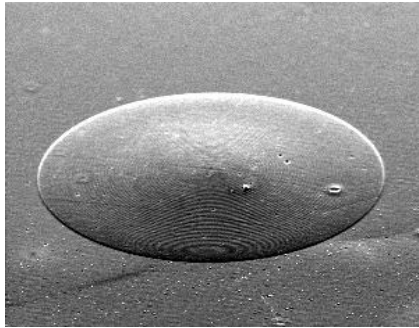


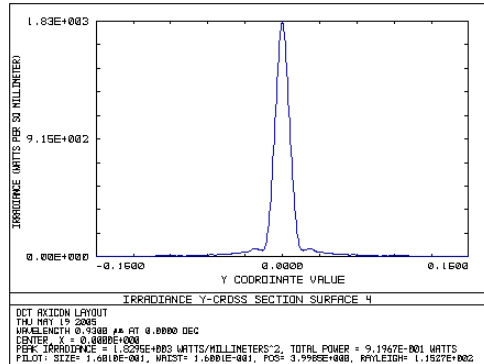
Fig.5 Point spread functions at focal planes of (a) 1mm (b) 1.8mm (c) 2.6mm from the point P shown in Fig. 4

4. Axicon fabrication and experiment

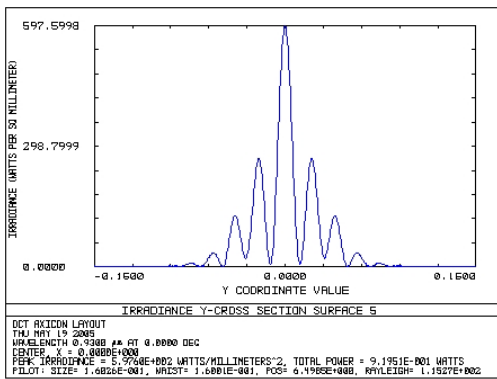
We fabricated an $800\mu\text{m}$ diameter axicon lens on silica wafer. An axicon phase mask pattern was written into Polymethyl-methacrylate (PMMA) on an E-beam machine, and then used in a stepper as a phase mask to create an analog axicon profile on a silica wafer. It was then developed and etched into the silica wafer. The fabricated axicon picture is shown in Fig. 6(a). We also analyzed the etched axicon pattern on the silica wafer with the Zygo interferometer to generate polynomial curve-fitting coefficients from the fabricated analog profile data. Then the curve-fitting data was placed into an optical system design software to perform simulations to get beam profiles shown in Fig 6(b), (c), and (d) over the DOF. The fabricated axicon lens has about a 3 degrees axicon angle and the corresponding DOF and central lobe size ρ_0 of beam profile are given by 15mm and $13\mu\text{m}$ with Eq. (1) and Eq. (2).



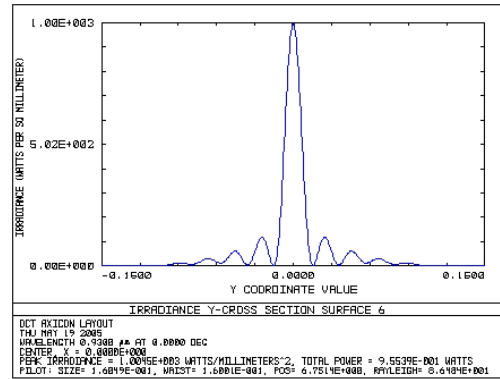
(a)



(b)



(c)



(d)

Fig.6. (a) SEM picture of the fabricated axicon, simulation of the beam pattern at (b) the start of the depth-of-focus (c) the middle of the depth-of-focus (d) the end of the depth-of-focus

The fabricated axicon lens was incorporated into the sample arm of an FD OCT interferometer to test its performance. FD OCT has attracted significant interest because of its improved sensitivity and imaging speed when compared to time domain OCT (TD-OCT).¹⁰ In FD OCT the axial information is derived from the spectrum of the interferometer output. The schematic diagram of the system is shown in Fig. 7. The FD OCT system consists of a broad bandwidth (i.e. 120nm at full-width-at-half-maximum centered at 800nm) Titanium:Sapphire laser, a commercial spectrometer with a CCD array, and a 80/20 fiber coupler which makes two arms of the interferometer. The 80% beam from the coupler is collimated and then incident on the axicon lens. The light is then focused on the sample. The other 20% beam is reflected by a mirror through the Fourier domain optical delay line in the reference arm whose main function is to control the overall dispersion in the system.¹¹

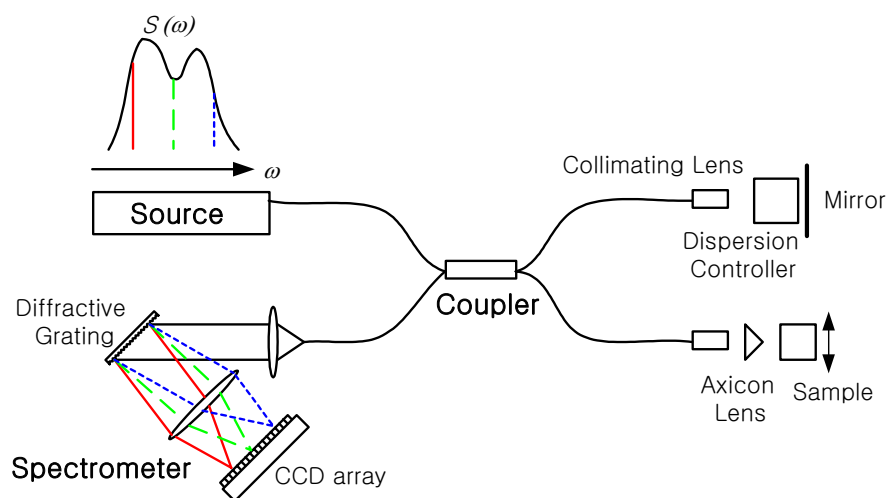


Fig. 7. Schematic diagram of a Fourier-domain OCT with an axicon as a focusing lens in the sample arm.

We first measured the intensity profile of the collimated beam before the focusing lens as shown in Fig. 8 and then measured the beam profile after passing through either the axicon lens or the spherical lens as a function of the distance from the lens. The collimated beam diameter was around $800\mu\text{m}$ and its profile was shaped as a Gaussian as shown in Fig. 8.

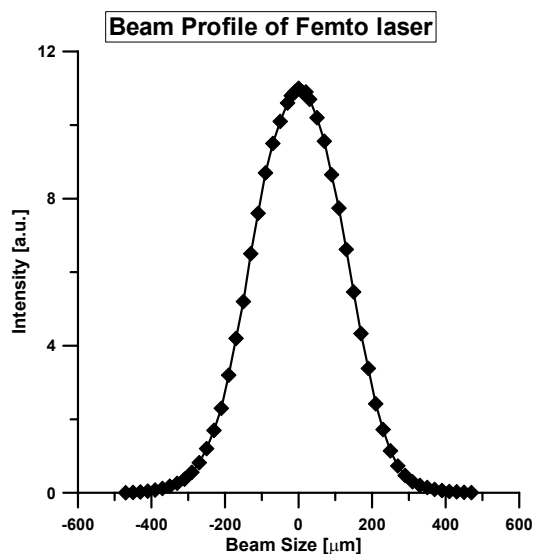


Fig. 8. Intensity profile of the collimated beam before the axicon lens.

The collimated beam was incident on an $800\mu\text{m}$ diameter axicon lens and the beam profiles at different planes from the axicon apex were measured as shown in Fig. 9(a). The geometrical DOF was almost 15mm which was estimated in Section 2, and the central lobe sizes were constant of value $13\mu\text{m}$ over the DOF. The peak intensity was decreased as the measured plane is moved away from the axicon lens because the incident beam was Gaussian in shape, which can be understood by considering Fig. 2 and how different beam heights are being imaged with the axicon. For comparison with a conventional lens we measured the beam profiles at different distances from the focal planes of an 8mm focal length spherical lens as shown in Fig. 9(b). The full width of the beam profile at the nominal focus plane by the

spherical lens was computed to be $10\mu\text{m}$. Although the beam width was better than that of the axicon lens at the focal plane, the beam width at 2mm away from the focal plane was found to be around $200\mu\text{m}$ which is highly broadened compared to that of the axicon lens.

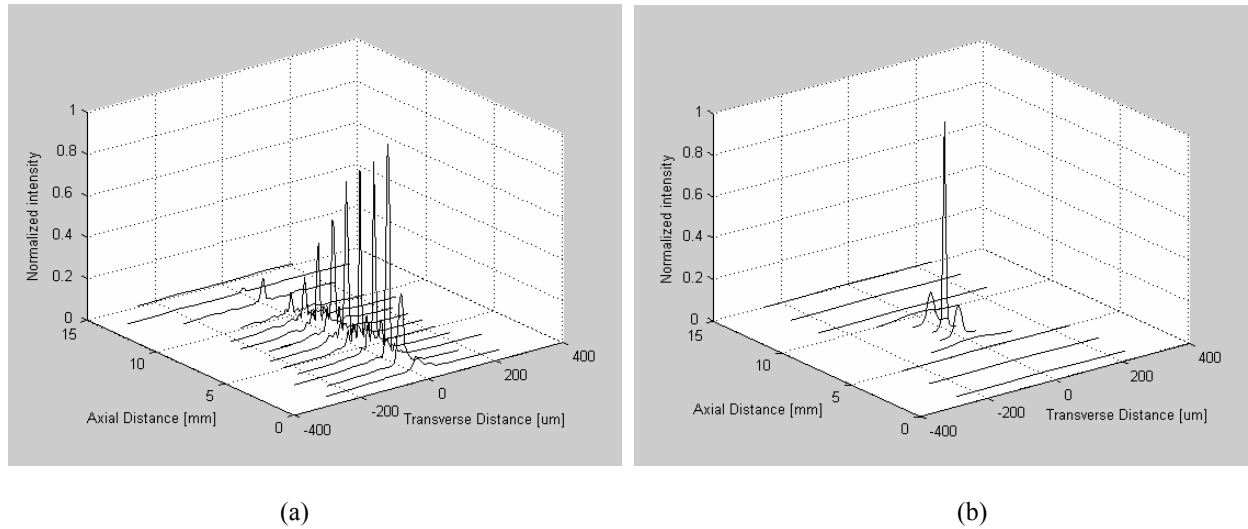


Fig. 9. Beam intensity profile after (a) an axicon lens (b) a spherical lens according to the distance from the lens

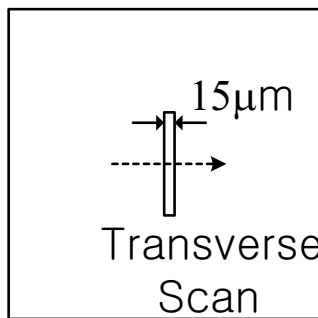
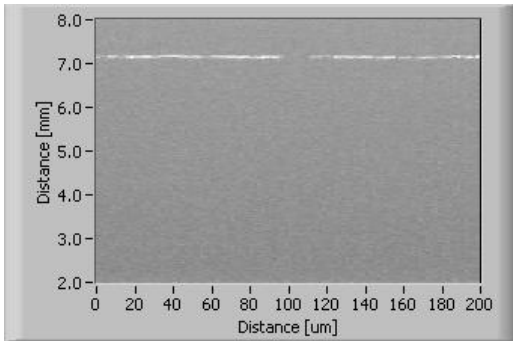
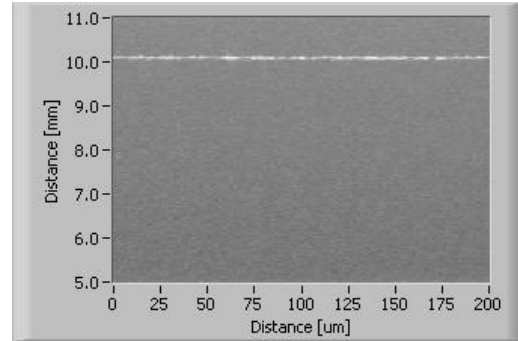


Fig. 10. A $15\mu\text{m}$ slit

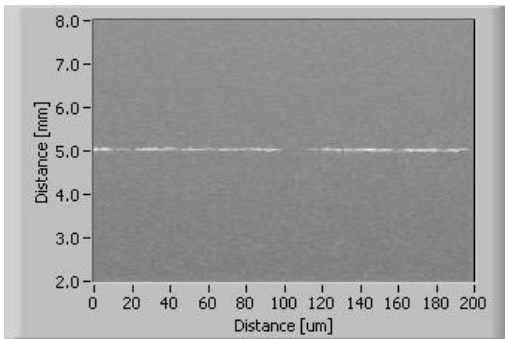
We imaged a $15\mu\text{m}$ slit shown in Fig 10 at three different distances from the lens for both an axicon lens and a spherical lens. Fig. 11(a), (c), (e) are the OCT images of the slit at the distances of 7mm, 5mm, and 3mm away from an axicon lens. Fig. 11(b), (d), (f) are the OCT images of the slit at the distances of 10mm, 8mm, and 6mm away from a spherical lens. The $15\mu\text{m}$ slit was imaged at 7mm, 5mm, and 3mm as shown in Fig. 11(a), (c), (e) while the spherical lens has an ability to resolve the slit only at a single focal plane as shown in Fig. 11(d). Results show good correlation between the sharpness of the point spread function and the ability to resolve the slit hole which is clearly observed in Figs. 11(a), (c), and (e).



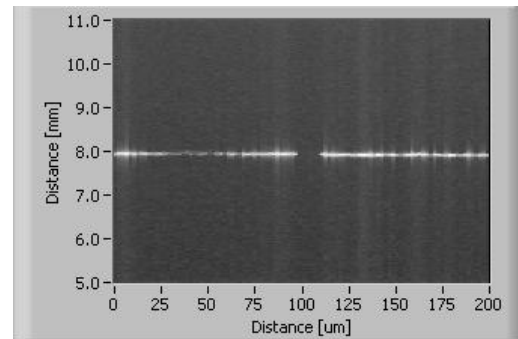
(a)



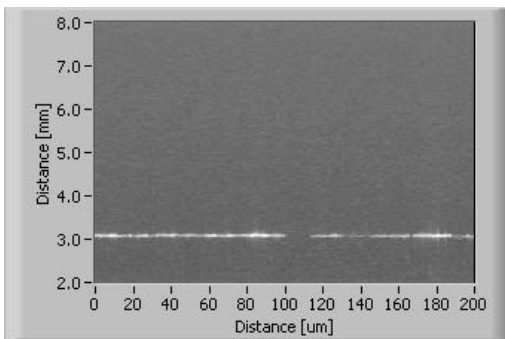
(b)



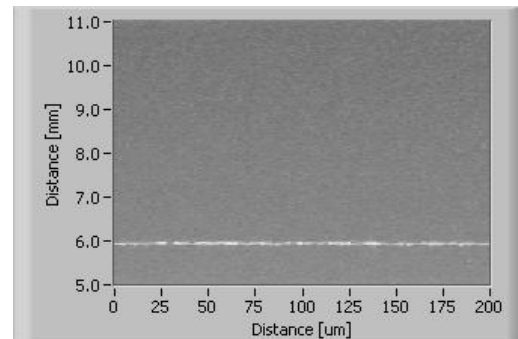
(c)



(d)



(e)



(f)

Fig.11. OCT images of a 15 μ m slit transversally scanned at distances of (a) 7mm, (c) 5mm, and (e) 3mm away from an axicon lens and (b) 10mm, (d) 8mm, and (f) 6mm away from a spherical lens

5. Conclusion

In this paper, we presented the design of a 2mm catheter for optical coherence endoscopy with a resolution of less than 5 micron across a DOF of about 1.6mm. An axicon lens was fabricated and tested in the laboratory. We demonstrated the impact of an axicon lens on the lateral resolution in OCT compared to a conventional lens. An axicon lens incorporated in OCT can render a constant high lateral resolution over long depths of focus compared with the conventional lens which can image only short depth ranges with high lateral resolution.

Acknowledgements

This research was supported in part by the Florida Photonics Center of Excellence, the NSF IGERT program, the UCF Presidential Instrumentation Initiative, and the DARPA & NSF PTAP program. We thank Optical Research Associates for the student license of Code V and their support to travel to IODC.

References

1. D. Huang, E. A. Swanson, C. P. Lin, J. S. Schuman, W. G. Stinson, W. Chang, M. R. Hee, T. Flotte, K. Gregory, C. A. Pulifito, and J. G. Fujimoto, "Optical coherence tomography," *Science* 254, 1178-1181 (1991).
2. Zhihua Ding, Hongwu Ren, Yonghua Zhao, J. Stuart Nelson, and Zhongping Chen, "High-resolution optical coherence tomography over a large depth range with an axicon lens," *Optics Letters* 27, 243-245 (2002).
3. W. Drexler, U. Morgner, F. X. Kortner, C. Pitris, S. S. Boppart, X. D. Li, E. P. Ippen, and J. G. Fujimoto, "In vivo ultrahigh-resolution optical coherence tomography," *Optics Letters* 24, 1221-1223 (1999).
4. R. Leitgeb, C. K. Hitzenberger, and A. F. Fercher, "Performance of fourier domain vs. time domain optical coherence tomography," *Optics Express* 11, 889-894 (2003), <http://www.opticsexpress.org>.
5. Anna Burvall, Katarzyna Kolacz, Zbigniew Jaroszewicz, and Ari T. Friberg, "Simple lens axicon," *Applied Optics* 43, 4838-4844 (2004).
6. M. Honkanen and J. Turunen, "Tandem systems for efficient generation of uniform-axial-intensity Bessel fields," *Opt. Commun.* 154, 368-375 (1998).
7. A. T. Friberg, "Stationary-phase analysis of generalized axicons," *J. Opt. Soc. Am. A* 13, 743-750 (1996).
8. J. Durmin, "Exact solutions for nondiffracting beams," *J. Opt. Soc. Am. A* 4, 651-654 (1987).
9. A. Jain, and H. Xie, "An Electrothermal Microlens Scanner with Low-Voltage, Large-Vertical-Displacement Actuation," *IEEE Photonics Technology Letters*, Vol. 17, No. 9, pp. 1971-1973, September 2005.
10. R. Leitgeb, C. K. Hitzenberger, and A. F. Fercher, "Performance of fourier domain vs. time domain optical coherence tomography," *Optics Express* 11, 889-894 (2003), <http://www.opticsexpress.org>.
11. Kye-Sung Lee, A. Ceyhan Akcay, Tony Delemos, Eric Clarkson, and Jannick P. Rolland, "Dispersion control with a Fourier-domain optical delay line in a fiber-optic imaging interferometer," *Appl. Opt.* 44, 4009-4022 (2005).